

is observed that the  $\omega = 0$  ( $E = \hbar\nu = \hbar\omega$ ) solution of  $H_p''$  finds its counterpart in the  $\omega = 0$  solution of  $H_D$  (cf. Eq. (2.6.6)). In the first case it restores gauge invariance, the associated collective modes being pairing rotational bands. In the second it restores translational invariance, the associated collective modes being, in the case of a single nucleus of mass number  $A$ , the GDR and the uniform translation of the nucleus as a whole with inertia  $AM$ . In the case of a direct reaction, for example of the two-nucleon transfer process  $a (= b + 2) + A \rightarrow b + B (= A + 2)$ , the collective modes are the GDR of the different nuclei involved (**structure**), and the continuous evolution of the relative motion (with varying reduced masses let alone the uniform motion of the CM) of the reacting nuclei, for each partial wave (quantal) or impact parameter (semiclassical), from the initial (to the intermediate  $f (= b + 1) + F (= A + 1)$ ), to the final channel (**reaction**). This continuity reflects the constraint  $H = H_a + H_A = H_f + H_F = H_b + H_B$ , which, in e.g. the semiclassical approximation is implemented by second order diagonalization of the operators  $\exp(\sigma_1 + \sigma_2)$  (recoil) and  $\exp(i/\hbar\gamma(t))$  ( $Q$ -value) (cf. App. 5.C, Eq. (5.C.4)). In quantum mechanics (second order DWBA), it is implemented by diagonalizing  $v_{np}$  to second order perturbation, in terms of partial wave expansions of the wavefunctions of relative motion associated with the variety of channels involved in the reaction process (cf. Figs. 3.1.1 and 3.1.2), as well as the NFT diagrams displayed in Figs. 5.C.1 and 5.C.2 (jaggedy line). It is, of course, the concrete (microscopic) implementation of structure (cf. Eqs. 6.1.1–6.1.3 ( $^{11}\text{Li}$ ) and Table 6.2.1 (Sn-isotopes)) and reaction (cf. the equation given in Figs. (3.1.1) and (3.1.2) at the basis of the software COOPER, plus global optical potentials), which eventually allows to compare theory with experiment in terms of absolute cross sections (Fig. 6.B.2 ( $^{11}\text{Li}(p, t)^9\text{Li(gs)}$ ) and Fig. 4.2.1 ( $^{A+2}\text{Sn}(p, t)^A\text{Sn(gs)}$ ), which eventually validates or less, the soundness of the chain of concepts: spontaneous symmetry breaking  $\rightarrow$  restoration  $\rightarrow$  emergent properties, as a valid tool to individuate collective modes in particular, and new physics in general.

We note that in the above examples namely  $^{11}\text{Li}$  and Sn-isotopes, one is talking about dynamical ( $\omega \approx 0; 380 \text{ keV}$ ) and static ( $\omega = 0$ ) breaking of gauge invariance respectively essentially on equal footing. Arguably, one is allowed to do so in keeping with the central role fluctuations in general and pairing vibrations in particular, play in atomic nuclei around closed shells, specially around the  $N = 6$  magic number.

### 6.3 BCS-like nucleon-nucleon correlation (Cooper pair)

The specific probe to quantitative test how much BCS-like correlated are two nucleons (nucleon holes) moving on top of the Fermi surface (in the Fermi sea) and interacting through an attractive pairing force, nuclear embodiment of a Cooper pair and known as pair addition (pair removal) modes (Bohr, A. and Mottelson (1975), Bès, D. R. and Broglia (1966)), is through two-nucleon transfer processes, e.g. through a  $(p, t)$  ( $a (t, p)$ ) reaction, like e.g.  $^1\text{H} (^{11}\text{Li}, ^9\text{Li(gs)}) ^3\text{H}$  and  $(^{206}\text{Pb}(t, p) ^{208}\text{Pb})$ .

*validating*

*0.380 keV*

*in the case of the reaction  $^{206}\text{Pb}(t, p)^{208}\text{Pb}$*

Let us start discussing the second one. In Fig. 3.4.4 we show the predictions of the pairing vibrational model in comparison with the experimental data (Bjergaard, J. H. et al. (1966)). The calculations were carried out making use of the software COOPER and of the spectroscopic amplitudes collected in Tables 2.5.2 and 2.5.3, and corresponding to the RPA, X- and Y- amplitudes associated with  $^{208}\text{Pb}$  pair removal mode, i.e. describing the ground state of  $^{206}\text{Pb}$  (two holes interacting via a pairing force of constant matrix element, and allowed to move in the single-particle valence orbitals; cf. Table 2.4.1). The global optical parameters for the proton and the triton were taken from the experimental paper, while those of the deuteron channel needed in COOPER to work out the successive transfer amplitude was taken from An and Cai (2006). Theory (RPA) provides an overall account of the observations ( $\sigma = 0.52\text{mb}$  to be compared with the experimental finding  $0.68 \pm 0.24\text{ mb}$ ). *explained \*\*)*

The large cross section, also for the pair addition mode, that is, associated with the population of the two-phonon ( $2p - 2h$ ) pairing vibrational state of  $^{208}\text{Pb}$  ( $0^+$ ; 4.95 MeV) was interpreted in Bertsch, G. F. et al. (1967) in terms of the angular correlation between the two fermions (holes) displayed in figure 7 of this reference (cf. also Figs. 2.4 and 2.5 Brink, D. and Broglia (2005)). By plotting the modulus square of the two-hole wavefunction as a function of one coordinate leaving the other fixed (both lying on the z-axis) it was shown that while  $j^2(0)$  displays a symmetric distribution for  $\Omega_{12} = 0^\circ$  and  $180^\circ$ , the correlated state displays an angular enhancement at  $\Omega_{12} = 0^\circ$ , radially peaked on the nuclear surface.

The fact that in the analysis of Broglia and Riedel (1967) only simultaneous transfer was considered, corroborated the connection between pairing collectivity, closeness of the two nucleons and thus the large cross sections. A further corroboration seems to emerge from the fact that TD (neglect of ground state correlations), let alone the pure two-hole configuration  $|p_{1/2}^{-2}(0)\rangle$  gives rise to cross sections which are smaller than that predicted by the full correlated state (Fig. 3.4.4). Now, as can be seen from the inset of this figure, most of the absolute cross section arises from successive transfer, a sobering result. Within this context, let us now comment on the reaction  $^1\text{H}(^{11}\text{Li}, ^9\text{Li(gs)})^3\text{H}$ . As seen from the  $|\Psi(\mathbf{r}_1, \mathbf{r}_2)|^2$  plots of the halo Cooper pair wavefunction displayed in Figs. 2.6.3 and 6.1.3, the correlation between the two pairing interacting neutrons is evident. Similarly the lack of correlation of the pure, angular momentum coupled configurations  $|s_{1/2}^2(0)\rangle$  and  $|p_{1/2}^2(0)\rangle$ . Now, the theoretical results reported in Fig. 6.1.3 calculated making use of the NFT results (6.1.1)–(6.1.3) and the optical potentials of Tanihata, et al. (2008) (those of An and Cai (2006) for the deuteron channel) reproduced the observations within the experimental findings. Again in this case, most of the absolute two-nucleon transfer differential cross section is connected with successive transfer (cf. Figs. 6.B.2 and 6.B.3). But not only this. While in the present case the absolute cross section associated with the pure  $|p_{1/2}^2(0)\rangle$  configuration is about an order of magnitude smaller than that associated with the full wavefunction (and thus also experiment), as observed in connection with  $^{206}\text{Pb}(t, p)^{208}\text{Pb}(\text{gs})$ , that as-

*\*) An and Cai (2006)*

*\*\*) Bertsch et al (1967); see also Figs. 2.4 and 2.5 Brink, D. and Broglie (2005)*

*\*\*\*) Broglie and Riedel (1967).*

*halo*

*and coverness \*\*\**

*\*\*\*\*)  
tanihata  
et al (2008)*

as far as two-nucleon transfer  
absolute cross section  
is concerned

sociated with the  $|s_{1/2}^2(0)\rangle$  pure configuration overpredicts the data by an order of magnitude. This is in spite of the fact that, as seen from the left, top corner of the two-dimensional plot of this configuration (Fig. 6.1.3), the two nucleons are as far as they can be from each other. This result is due to the fact that the  $p_{1/2}^2(0)$  is a cold configuration (small  $S = 0$  component) while  $s_{1/2}^2(0)$  is a hot one (large  $S = 0$  component) (e.g. Broglia, R. A. et al. (1972) and refs. therein). Furthermore, the fact that the density associated with the two halo neutrons is much lower than that associated with the core nucleons, implies that in average, they are further away from each other than nucleons in a "normal" ( $R_0 = 1.2A^{1/3}$  fm-like) nucleus (Sect. 3.2 Eqs. (3.2.21)-(3.2.27)). This fact allows them to lower their relative momentum, without for that loosing their coherence, nor the associated conspicuous ability to tunnel as a single entity (absolute  $(p, t)$  cross section). In fact  $\sigma(^{11}\text{Li}(p, t)^9\text{Li(gs)}) \approx 5.7 \pm 0.9$  mb (cf. Fig. 6.B.2), to be compared to  $\sigma(^{206}\text{Pb}(t, p)^{208}\text{Pb(gs)}) \approx 0.68 \pm 0.24$  mb.

Summing up, the two halo neutrons of  $^{11}\text{Li}$  are likely to provide a paradigm of nuclear Cooper pairs: delicate (soap bubble like) extended objects with low relative momentum behaving in tunneling processes as an entity, in keeping with their unique emergent property: generalized gauge rigidity, equally present in collective pairing vibrational (dynamic) as pairing rotational situations (within this context also Apps. 6.G, 6.H and 6.I).

One can conclude this Section by stating that its title could as well having been: "prejudices revisited". Prejudices that the senior author of this monograph have helped to foster for a long time.

## Appendix 6.A Bootstrap particle-phonon mechanism to spontaneously break gauge invariance

In this Appendix we discuss a gedanken experiment, aimed at clarifying the bootstrap pairing mechanism resulting in the binding of the neutron halo of  $^{11}\text{Li}$ .

### 6.A.1 Gedanken eksperiment

Let us assume that one shines a low-energy neutron beam on a  $^9\text{Li}$  target. If these neutrons felt only the associated single-particle mean field, they will go by essentially as fast as they came in. However, part of the time pairs of these neutrons will bound themselves in presence of phonon (bosonic) excitations of quadrupole and of (pygmy) dipole character, produced also by the field the two neutron create themselves. The first of these collective modes is associated with vibrations of the (even)  $^8\text{He}$  core, the second resulting from the sloshing back and forth of the strongly non-local field of two (passing by) neutrons of the beam, together with the neutrons, and against the protons, of the core. Such possibility implies that, for a short time, of the order of the traversal time, the two (unbound) neutrons will move in a gas of virtual bosonic excitations, also made out of dipole pygmy reso-

→ \*)

y  
pygmy

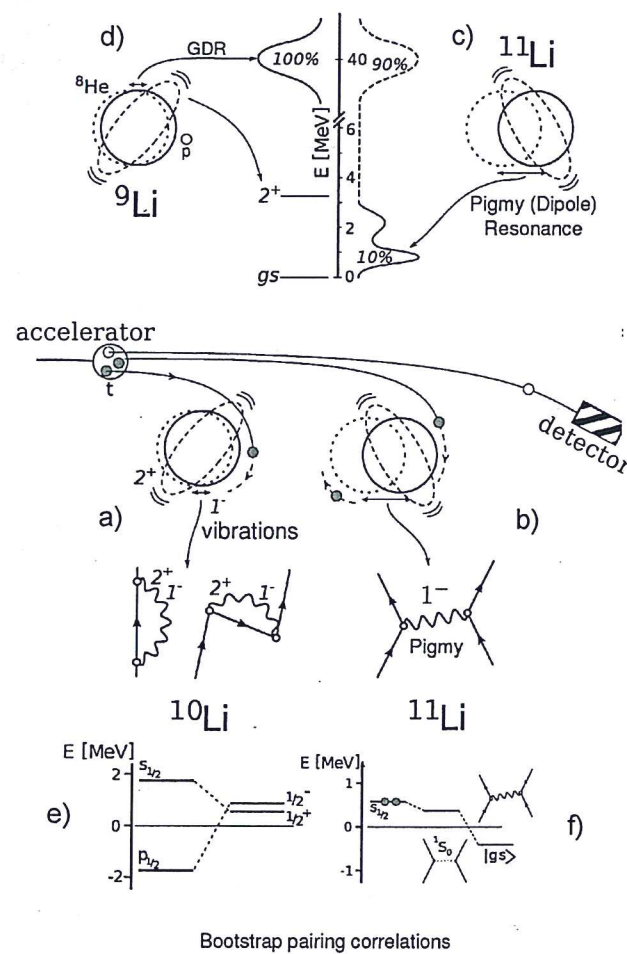
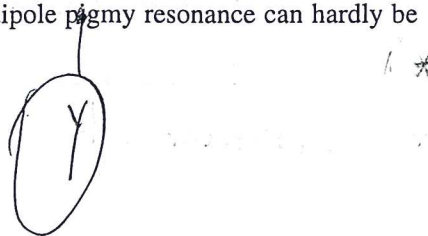


Figure 6.A.1: Schematic representation of the collective quadrupole and dipole response of lithium isotopes, and of a  $(t, p)$  reaction (in the text one reasons in terms of flux of low energy neutrons) in which two neutrons are transferred to  $^{9}\text{Li}$  (see also Fig. 6.1.3).

nances. Consequently, they can get dressed becoming heavier (lighter), as well as getting correlated by exchanging these bosonic collective vibrations. The first phenomenon is associated, as discussed above, with phononic backflow (Pauli principle upflow) leading to  $^{10}\text{Li}$ -like quasi-bound ( $s$ -wave) and resonant ( $p$ -wave) dressed single-particle states displaying parity inversion. The second phenomenon, mediated by phonon exchange between halo neutrons, contributes in a major way to the glue which binds the neutron halo Cooper pair to the  $^{9}\text{Li}$  core. Within the above scenario, one can posit that the  $^{11}\text{Li}$  dipole pigmy resonance can hardly be



viewed but in symbiosis with the  ${}^9\text{Li}$  halo neutron pair addition mode. The above described bootstrap phonon-exchange mechanism can be viewed as a novel microscopic embodiment of the Bardeen-Pines-Frölich-like processes to spontaneously break gauge invariance<sup>1</sup>.

To conclude, let us comment on Fig. 6.A.1. As said above, (a) the dressing of single-particle levels by collective vibrations and (b) the renormalization of the bare  $NN$ -interaction, in particular of the pairing interaction, through the exchange of these modes between nucleons moving in time reversal states lying close to the Fermi energy, play a central role in nuclear structure. In particular, in the case of the single Cooper pair system  ${}^{11}\text{Li}$ , most of the glue is provided by the exchange of the pigmy resonance, namely a low-lying isovector dipole vibration. The pigmy resonance (c) is a chunk of the GDR of the core  ${}^9\text{Li}$  (d) and arises from radial inhomogeneous damping. This mode is intimately related to the spontaneous symmetry breaking of space homogeneity associated with the fact that the center of mass of a finite system like the atomic nucleus, specifies a privileged position in space. While  ${}_3^9\text{Li}_6$  is bound,  ${}_3^9\text{Li}_7$  is not. (e) through renormalization processes, the  $p_{1/2}$  bound state is shifted to higher energies from that predicted by a standard mean field potential, while the  $s_{1/2}$  continuum state is lowered to an energy closer below that of the  $p_{1/2}$  state. (f) While the screened bare pairing interaction is subcritical, the exchange of vibrations between the halo neutrons is able to, weakly, bind the system.

### Appendix 6.B

**Table 1 PRL**

Alternative processes  
to populate  $|{}^9\text{Li}(1/2^-)\rangle$

The  $1/2^-$  (2.69 MeV) first excited state of  ${}^9\text{Li}$  can in principle, not only be populated through a two-particle transfer process, but also through a break up process in which one (see Fig. 6.B.1(f)), or both neutrons (see Fig. 6.B.1(g)) are forced into the continuum for then eventually one of them to fall into the  $1p_{3/2}$  orbital of  ${}^9\text{Li}$  and excite the quadrupole vibration of the core (Potel et al. (2010)), in keeping with the fact that the main RPA amplitude of this state is precisely  $X(1p_{3/2}^{-1}, 1p_{1/2})(\approx 1)$  (cf. ref Barranco, F. et al. (2001)). The remaining channel populating the first excited state of  ${}^9\text{Li}$  is associated with an inelastic process (see Fig. 6.B.1(h)): two-particle transfer to the ground state of  ${}^9\text{Li}$  and Final State (inelastic scattering) Interaction (FSI) between the outgoing triton and  ${}^9\text{Li}$  in its ground state, resulting in the inelastic excitation of the  $1/2^-$  state. *NFT (developed by Barranco and coworkers)*

Making use of the wavefunctions of Barranco, F. et al. (2001) and of a software developed on purpose to take into account microscopically all the different processes mentioned above, that is 9 different reaction channels (cf. caption to Table 6.B.1) and continuum states up to 50 MeV of excitation energy, the corresponding transfer amplitudes and associated probabilities  $p_i$  were calculated.

<sup>1</sup>Bootstrapping or booting. The term is often attributed to Rudolf Erich Raspe's story The surprising Adventures of Baron Münchhausen, where the main character pulls himself out of a swamp by his hair. Early 19th century USA: "pull oneself over a fence by one's bootstraps"

\*) Potel et al (2010)

\*\*) Barranco et al (2001)

In Table 6.B.1 are displayed the probabilities  $p_l = |S_l^{(c)}|^2$  associated with each of the processes discussed above, where the amplitude  $S_l^{(c)}$  is related to the total cross section associated with each of the channels  $c$  by the expression (Satchler, 1980; Landau and Lifshitz, 1981).

$$\sigma_c = \frac{\pi}{k^2} \sum_l (2l+1) |S_l^{(c)}|^2, \quad (6.B.1)$$

$k$  being the wave number of the relative motion between the reacting nuclei.

In keeping with the small values of  $p_l$ , in what follows we take into account the interference between the contributions associated with the different reaction paths making use of second order perturbation theory, instead of a coupled channel treatment (e.g. Ascuitto and Glendenning (1969) Tamura, T. et al. (1970) Khoa and von Oertzen (2004) Keeley et al. (2007) Thompson (1988)). In particular in the case of the  $1/2^-$  (2.69 MeV) first excited state of  ${}^9\text{Li}$ ,

$$\frac{d\sigma}{d\Omega}(\theta) = \frac{\mu^2}{16\pi^3 \hbar^4} \left| \sum_l (2l+1) P_l(\theta) \sum_{c=2}^5 T_l^{(c)} \right|^2, \quad (6.B.2)$$

where  $\mu$  is the reduced mass and  $T_l^{(c)}$  are the transition matrix elements (in the DWBA Satchler (1980)) associated with the different channels and for each partial wave of DWBA.

Making use of all the elements discussed above, multistep transfer (see e.g. Bayman and Chen (1982), Igarashi et al. (1991), Bayman and Feng (1973) as well as Broglia and Winther (2004)), breakup and inelastic channels were calculated, and the results displayed in Figs. 6.B.2 and 6.B.3 and in Table 6.B.1. Theory provides an overall account of the experimental findings. In particular, in connection with the  $1/2^-$  state, this result essentially emerges from cancellations and coherence effects taking place between the three terms contributing to the multistep two-particle transfer cross section (Fig. 6.B.3), tuned by the nuclear structure amplitudes associated with the process shown in Fig. 6.B.1 (e) as well as Eqs. (6.1.1)–(6.1.3). In fact, and as shown in Figs. 6.B.2 and 6.B.3, the contributions of break up processes and inelastic (Figs. 6.B.1(f),(g) and (h) respectively) to the population of the  $1/2^-$  (2.69 MeV) first excited state of  ${}^9\text{Li}$  are negligible as compared with the process depicted in Fig. 6.B.1(e). In the case of the breakup channel (Figs. 6.B.1(f) and 6.B.1(g)) this is a consequence of the low bombarding energy of the  ${}^{11}\text{Li}$  beam (inverse kinematics), combined with the small overlap between continuum (resonant) neutron  $p_{1/2}$  wavefunctions and bound state wavefunctions. In the case of the inelastic process (Fig. 6.B.1(h)), it is again a consequence of the relative low bombarding energy. In fact, the adiabaticity parameters  $\xi_C, \xi_N$  (see eqs. (IV.12) and (IV.14) of ref. Broglia and Winther (2004)) associated with Coulomb excitation and inelastic excitation in the  $t + {}^9\text{Li}$  channel are larger than 1, implying an adiabatic cutoff. In other words, the quadrupole mode is essentially only polarized during the reaction but not excited. The situation is quite different

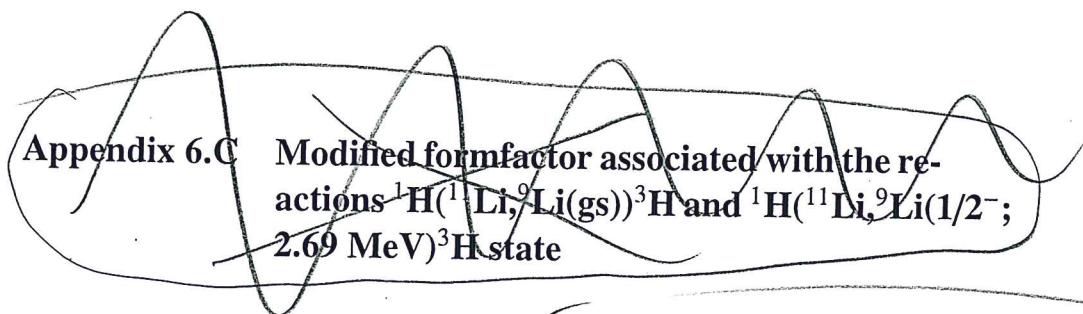
\*) Satchler 1980; Landau and Lifshitz 1981.

\*\*) See ↗

\*\*\*\*) ↗

\*\*\*\*\*) ↗

in the case of the intervening of the virtual processes displayed in Fig. 6.B.1 (b) and (c) leading to the population of the  $1/2^-$  state displayed in Fig. 6.B.1 (e). Being those off-the-energy shell processes, energy is not conserved, and adiabaticity gets profoundly modified.



## Appendix 6.D Software

*Answer to Ben Bayman question*

In this Appendix we provide a brief description of the numerical methods implemented in the code written to evaluate the differential cross sections. The two-nucleon transfer differential cross section is given by Eq. (5.1.4), so the principal task consist in calculating the transfer amplitudes  $T^{(1)}(\theta)$ ,  $T_{succ}^{(2)}(\theta)$  and  $T_{NO}^{(2)}(\theta)$  described in Eqs. 5.1.5a–5.1.5c, by numerically evaluating the corresponding integrals. The dimensionality of the integrals can be reduced by expanding in partial waves (eigenfunctions of the angular momentum operator) the distorted waves and wavefunctions present in the corresponding integrands. The resulting expressions are Eqs. (5.2.36) and (5.2.37) for  $T^{(1)}(\theta)$ , Eqs. (5.2.128), (5.2.129) and (5.2.130) for  $T_{succ}^{(2)}(\theta)$ , and Eqs. (5.2.154), (5.2.155) and (5.2.156) for  $T_{NO}^{(2)}(\theta)$ . The integrals are computed numerically with the method of Gaussian quadratures.

The one-dimensional (radial) functions appearing in the integrands are defined in a spatial grid up to a given maximum radius  $r_{max}$ . The bound state wavefunctions are obtained by numerical integration of the radial Schrödinger equation for a Woods-Saxon potential with a spin-orbit term. The parameters defining the shape of the potential are given as an input, while the depth is adjusted to reproduce the binding energy of the state under consideration. The resulting potential corresponding to the final (initial) nucleon bound state stands also for the interaction potential featured in the integrand in the prior (post) representation. The distorted waves are obtained by integrating the radial Schrödinger equation with positive energy from  $r = 0$  to  $r_{max}$ , and matching the solution with the corresponding Coulomb wave function at a given  $r = r_{match}$ , big enough to lie outside of the range of the nuclear interaction. The Woods-Saxon optical potentials used to obtain the distorted waves consist on a real Coulomb term, a real and imaginary volume terms, an imaginary surface term, and a real and imaginary spin orbit terms. The parameters needed to specify all those terms are given as an input.

*Gregory*

## 6.E. ARTICULO BELYAEV PAIRING VIBRATIONAL BAND BASED ON $N = 6.403$

~~Appendix 6.E Articulo Belyaev Pairing vibrational band based on  $N = 6$ .~~

~~Appendix 6.F Simple estimates revisited.~~

## Appendix 6.G Statistics.

Let us consider two identical particles moving in a one-dimensional harmonic oscillator. Let us assume that one is in the ground state and the other is in the first excited state. According to the superposition principle

$$\Phi(x_1, x_2) = \lambda\phi_1(x_1)\phi_0(x_2) + \mu\phi_0(x_1)\phi_1(x_2). \quad (6.G.1)$$

Let us calculate the correlation of these particles, that is, the quantity

$$C = \frac{\langle x_1 x_2 \rangle - \langle x_1 \rangle \langle x_2 \rangle}{\sqrt{(\langle x_1^2 \rangle - \langle x_1 \rangle^2)(\langle x_2^2 \rangle - \langle x_2 \rangle^2)}} \quad (6.G.2)$$

Let us start with

$$\begin{aligned} \langle x_1 x_2 \rangle &= \int dx_1 dx_2 (\lambda^* \phi_1^*(x_1) \phi_0^*(x_2) + \mu^* \phi_0^*(x_1) \phi_1^*(x_2)) \\ &\quad \times (x_1 x_2) (\lambda\phi_1(x_1)\phi_0(x_2) + \mu\phi_0(x_1)\phi_1(x_2)) \\ &= |\lambda|^2 \langle \phi_1 | x_1 | \phi_1 \rangle \langle \phi_0 | x_2 | \phi_0 \rangle + \lambda^* \mu \langle \phi_1 | x_1 | \phi_0 \rangle \langle \phi_0 | x_2 | \phi_1 \rangle \\ &\quad + \lambda \mu^* \langle \phi_0 | x_1 | \phi_1 \rangle \langle \phi_1 | x_2 | \phi_0 \rangle + |\mu|^2 \langle \phi_0 | x_1 | \phi_0 \rangle \langle \phi_1 | x_1 | \phi_1 \rangle \langle \phi_0 | x_1 | \phi_0 \rangle \langle \phi_1 | x_1 | \phi_1 \rangle \end{aligned} \quad (6.G.3)$$

In keeping with the fact that

$$\langle \phi_1 | x | \phi_1 \rangle = \langle \phi_0 | x | \phi_0 \rangle = 0, \quad (6.G.4)$$

and

$$\langle \phi_0 | x | \phi_1 \rangle = \langle \phi_1 | x | \phi_0 \rangle = \sqrt{\frac{\hbar\omega}{2C}}, \quad (6.G.5)$$

one obtains

$$\langle x_1 x_2 \rangle = \left( \frac{\hbar\omega}{2C} \right) \Re(\lambda^* \mu). \quad (6.G.6)$$

And

$$\sqrt{-} = \left( \frac{\hbar\omega}{2C} \right), \quad (6.G.7)$$

for the denominator of Eq. (6.G.2). From the above results the correlation function between particle 1 and 2 is

$$C = \frac{2C}{\hbar\omega} \langle x_1 x_2 \rangle = 2\Re(\lambda^* \mu) = \begin{cases} 1 & (\lambda = +\mu = \frac{1}{\sqrt{2}}) \\ -1 & (\lambda = -\mu = \frac{-1}{\sqrt{2}}) \end{cases} \quad (6.G.8)$$

It is of notice that, in quantum mechanics, average values imply the mean outcome of a large number of experiments. In this case, of the (simultaneous) measure of the position of the two particles (*Basdevant and Dalibard (2005)*).

## Appendix 6.H Correlation length and quantity parameter.

The correlation length can be defined as

$$\xi = \frac{\hbar v_F}{2\Delta} \approx \frac{\hbar^2 k_F}{m 2\Delta} \quad (6.H.1)$$

where the Fermi momentum in the case of stable nuclei lying along the stability valley is

$$k_F \approx 1.36 \text{ fm}^{-1}. \quad (6.H.2)$$

Thus,

$$\xi = 20 \text{ MeV fm}^2 \times \frac{1.36}{\Delta} \text{ fm}^{-1} \approx \frac{27}{\Delta} \text{ fm}, \quad (6.H.3)$$

and,

$$\xi \approx 27 \text{ fm}, \quad (\Delta \approx 1 \text{ MeV}). \quad (6.H.4)$$

Let us now define,

$$k_F \approx \frac{a}{\xi} = 1.36 \text{ fm}^{-1} \quad (6.H.5)$$

obtaining,

$$a \approx 37; \quad k_F \approx \frac{37}{\xi}. \quad (6.H.6)$$

One can then write,

$$1 = \left( \frac{\hbar^2}{m\xi^2} \right) \left( \frac{1}{2\Delta} \right) 37 = q \times 37, \quad (6.H.7)$$

where the quantity parameter is, in the present case,

$$q \approx 0.03. \quad (6.H.8)$$

# Appendix G. I Multipole pairing vibrations; open problem concerning multipole

(B)

p. 405 a

## 6.H. CORRELATION LENGTH AND QUANTITY PARAMETER.

That is, the two partner nucleons are, in the Cooper pair, rigidly anchored.

We now consider  $^{11}\text{Li}$ , and calculate  $k_F$  (neutrons) with the help of the Thomas-Fermi model,

$$k_F = \left( 3\pi^2 \frac{8}{\frac{4\pi}{3}(4.58)^3} \right)^{1/3} \text{fm}^{-1} \approx \frac{(18\pi)^{1/3}}{4.58} \text{fm}^{-1} \approx 0.84 \text{ fm}^{-1}. \quad (6.H.9)$$

The correlation length is,

$$\xi \approx \frac{\hbar^2}{m} \frac{k_F}{2E_{corr}} \approx 20 \text{ MeV fm}^{-1} \approx 42 \text{ fm}, \quad (6.H.10)$$

and

$$k_F = \frac{a}{\xi} \approx \frac{a}{42 \text{ fm}} = 0.84 \text{ fm}^{-1}; \quad a \approx 35; \quad k_F = \frac{35}{\xi}, \quad (6.H.11)$$

leading to

$$1 = \left( \frac{\hbar^2}{m\xi^2} \right) \left( \frac{1}{2E_{corr}} \right) 35 = q \times 35, \quad (6.H.12)$$

and of the resulting quantity parameter,

$$q \approx 0.03. \quad (6.H.13)$$

It is of notice that this result is but an alternative embodiment of the relation (3.3.8). Now, one could argue that both (3.3.8) and (6.H.13) (as well as (6.H.8) for stable nuclei), are just a manifestation of (6.G.8). That there is more to it is forcefully expressed by the fact that, selecting  $|s_{1/2}^2(0)\rangle$  ( $|p_{1/2}^2(0)\rangle$ ) as the Cooper pair of  $^{11}\text{Li}$  leads to absolute two-particle transfer cross sections which are about one order of magnitude larger (smaller) than the observed cross section (see Fig. 6.1.3). The fact that the NFT result (6.1.1)–(6.1.3) with its unusual pygmy binding and parity inversion cloaking mechanism reproduces observations within experimental errors, underscores the central role played by structure on Cooper pair tunneling, through the emergent property of generalized pairing rigidity ~~partners~~

Summing up pairing, both bare  $NN$ - and long range induced interaction changes the statistics of the elementary modes from fermionic to bosonic and, at the same time, the value of the quantity parameter from  $q \approx 1$  to  $q \ll 1$  (delocalized  $\rightarrow$  rigidly anchored to the Cooper pair) thus leading to a generalized gauge rigidity, the detailed renormalizing and dressing mechanisms ultimately deciding on the soundness and applicability of the description under discussion. The fact that in working out the reaction mechanism one uses, for practical reasons, a single-particle basis (second order DWBA corrected by non-orthogonality), reconstructing the interweaving of these particles with the collective modes in term of sums over virtual states, does not alter the physics embodied in the NFT solutions. Rather, it provides its confirmation (Fig. 6.1.3).

Appendix 6.J Asymmetry between particle and hole phase spaces: NFT at the level of hundred keV.

6.I.1 Cooper pair vortex  
405

6.I.2 Deformation in 2D-square in the rms of multipole pair vibrations

### Appendix 6.I - $k$ -mass in $^{11}\text{Li}$ and Pauli principle.

#### Bibliography

- ✓ H. An and C. Cai. Global deuteron optical model potential for the energy range up to 183 MeV. *Phys. Rev. C*, 73:054605, 2006.
- ✓ P. W. Anderson. Random-phase approximation in the theory of superconductivity. *Phys. Rev. Lett.*, 112:1900, 1958.
- ✓ R. J. Asciutto and N. K. Glendenning. Inelastic processes in particle transfer reactions. *Physical Review*, 181:1396, 1969.
- ✓ F. Barranco, R. A. Broglia, G. Gori, E. Vigezzi, P. F. Bortignon, and J. Terasaki. Surface vibrations and the pairing interaction in nuclei. *Phys. Rev. Lett.*, 83: 2147, 1999.
- ✓ Barranco, F., P. F. Bortignon, R. A. Broglia, G. Colò, and E. Vigezzi. The halo of the exotic nucleus  $^{11}\text{Li}$ : a single Cooper pair. *Europhys. J. A*, 11:385, 2001.
- ✓ J. L. Basdevant and J. Dalibard. *Quantum Mechanics*. Springer, Berlin, 2005.
- ✓ G. Bassani, N. M. Hintz, C. D. Kavaloski, J. R. Maxwell, and G. M. Reynolds. ( $p, t$ ) Ground-State  $L = 0$  Transitions in the Even Isotopes of Sn and Cd at 40 MeV,  $N = 62$  to 64. *Phys. Rev.*, 139:B830, 1965.
- ✓ B. F. Bayman and J. Chen. One-step and two-step contributions to two-nucleon transfer reactions. *Phys. Rev. C*, 26:1509, 1982.
- ✓ B. F. Bayman and B. H. Feng. Monte Carlo calculations of two-neutron transfer cross sections. *Nuclear Physics A*, 205:513, 1973.
- ✓ Bennaceur, K., J. Dobaczewski, and M. Ploszajczak. Pairing anti-halo effect. *Physics Letters B*, 496:154, 2000.
- ✓ Bertsch, G. F. and R. A. Broglia. Giant resonances in hot nuclei. *Physics Today*, 39 (8):44, 1986.
- ✓ Bertsch, G. F., R. A. Broglia, and C. Riedel. Qualitative description of nuclear collectivity. *Nucl. Phys. A*, 91:123, 1967.
- ✓ Bès, D. R. and R. A. Broglia. Pairing vibrations. *Nucl. Phys.*, 80:289, 1966.
- ✓ Bjerregaard, J. H., O. Hansen, Nathan, and S. Hinds. States of  $^{208}\text{Pb}$  from double triton stripping. *Nucl. Phys.*, 89:337, 1966.
- ✓ N. Bogoljubov. On a new method in the theory of superconductivity. *Il Nuovo Cimento*, 7:794, 1958.

## BIBLIOGRAPHY

distorted-wave Born approximation calculations. *Phys. Rev. C*, 83:044614, 2011.

✓ Guazzoni, P., L. Zetta, A. Covello, A. Gargano, B. F. Bayman, G. Graw, R. Hertenberger, H. F. Wirth, T. Faestermann, and M. Jaskola. High resolution spectroscopy of  $^{112}\text{Sn}$  through the  $^{114}\text{Sn}(p, t)^{112}\text{Sn}$  reaction. *Phys. Rev. C*, 85:054609, 2012.

✓ I. Hamamoto and B. R. Mottelson. Pair correlation in neutron drip line nuclei. *Phys. Rev. C*, 68:034312, 2003.

✓ Hamamoto, I. and B. R. Mottelson. Weakly bound  $s_{1/2}$  neutrons in the many-body pair correlation of neutron drip line nuclei. *Phys. Rev. C*, 69:064302, 2004.

✓ M. Igarashi, K. Kubo, and K. Yagi. Two-nucleon transfer mechanisms. *Phys. Rep.*, 199:1, 1991.

✓ N. Keeley, R. Raabe, N. Alamanos, and J.-L. Sida. Fusion and direct reactions of halo nuclei at energies around the Coulomb barrier. *Prog. Nucl. Part. Phys.*, 59: 579, 2007.

✓ D. T. Khoa and W. von Oertzen. Di-neutron elastic transfer in the  $^4\text{He}^6\text{He}$ ,  $^6\text{He}^4\text{He}$  reaction. *Physics Letters B*, 595:193, 2004.

✓ L. Landau and L. Lifshitz. *Quantum Mechanics, 3rd ed.* Butterworth-Heinemann, 1981.

✓ G. Potel, F. Barranco, E. Vigezzi, and R. A. Broglia. Evidence for phonon mediated pairing interaction in the halo of the nucleus  $^{11}\text{Li}$ . *Phys. Rev. Lett.*, 105:172502, 2010.

✓ G. Potel, A. Idini, F. Barranco, E. Vigezzi, and R. A. Broglia. Nuclear Field Theory predictions for  $^{11}\text{Li}$  and  $^{12}\text{Be}$ : shedding light on the origin of pairing in nuclei. *Yad. Fiz.*, *in press*: arXiv:1210.5085 [nucl-th], 2014.

✓ Potel, G., A. Idini, F. Barranco, E. Vigezzi, and R. A. Broglia. Cooper pair transfer in nuclei. *Rep. Prog. Phys.*, 76:106301, 2013a.

✓ Potel, G., A. Idini, F. Barranco, E. Vigezzi, and R. A. Broglia. Quantitative study of coherent pairing modes with two-neutron transfer: Sn isotopes. *Phys. Rev. C*, 87:054321, 2013b.

✓ G. Satchler. *Introduction to Nuclear Reactions*. Mc Millan, New York, 1980.

✓ J. Schrieffer. *Superconductivity*. Benjamin, New York, 1964.

✓ Schrieffer, J. R. Macroscopic quantum phenomena from pairing in superconductors. *Physics Today*, 26 (7):23, 1973.

ref.  
atom. Nucl.